

FOUR-QUADRANT TOTAL TO STATIC CHARACTERISTICS OF AN AXIAL FLOW COMPRESSOR

A. Gill, L. M. Beviss-Challinor, T. W. von Backström* and T. M. Harms
Department of Mechanical Engineering
University of Stellenbosch
South Africa

ABSTRACT

An axial flow compressor operating under near-design conditions exhibits rotation, flow and pressure difference between inlet and outlet and rotation in the expected directions. However, during abnormal operating conditions, some of these properties may reverse in direction. In this paper, the experimentally determined four-quadrant compressor maps for pressure-rise, torque and efficiency for a three-stage, low speed axial flow compressor are presented. Six possible modes of operation were identified and investigated; two compressor-like modes in the first and third quadrants, and two turbine-like modes and two highly dissipative modes in the second and fourth quadrants. This paper presents total to static pressure and torque coefficient characteristics for operation in all six quadrants, including reverse rotation modes, as well as efficiency characteristics where appropriate. Results are compared with those of previous researchers for reverse flow, positive rotation operation. The zero-rotation total to static pressure characteristic has been experimentally determined, and found to take the form of an S-shaped curve passing through the second and fourth quadrants, separating the turbine and dissipative modes in both the second and fourth quadrants.

NOMENCLATURE

A	compressor annulus sectional area
P	pressure
r_{tip}	blade tip radius
T	torque
U	blade tip speed
ρ	density
ϕ	flow coefficient
ψ_{TS}	total to static pressure rise coefficient
τ	torque coefficient
ω	rotor angular velocity
subscripts	
0	stagnation condition
<i>in</i>	condition at compressor inlet
<i>out</i>	condition at compressor outlet

*Corresponding author: email at twvb@sun.ac.za

INTRODUCTION

An axial flow compressor operating under near-design conditions exhibits flow, pressure difference between inlet and outlet and rotation in the expected directions. However, during abnormal operating conditions, such as surge or windmilling in an aircraft engine, or a failure of a component upstream or downstream of the compressor in an industrial setting, one or more of these properties may reverse in direction. By extending the horizontal and vertical axes of the total to static pressure rise, torque and efficiency maps of a compressor in the negative direction, these abnormal modes may be displayed as constant-speed characteristics in the second, third and fourth quadrants, the first quadrant representing the normal operational regime of the machine.

In this paper, the experimentally determined four-quadrant compressor maps for pressure-rise, torque and efficiency for a three-stage, low speed axial flow compressor are presented.

Six possible modes of operation were identified and investigated. If the rotor remains stationary while air is forced through the compressor in the design and reverse directions, the resulting zero-speed total to static pressure characteristic forms an S-shaped curve composed of two parabolic curves which join smoothly at the origin and pass through the second and fourth quadrants. Two modes occur in each of these quadrants, as both positive and negative rotation are possible, and are separated by the zero-rotation S-curve. Only one mode is possible in each of the first and third quadrants, as the zero-speed curve cannot pass through these quadrants; consequently negative rotation cannot occur in the first quadrant, nor positive rotation in the third. The areas of the compressor map occupied by each of the six modes are shown graphically in figure 1, together with the notation system for identifying each mode based on the sign or direction of five running conditions, namely flow rate (F), pressure (P), rotational speed (N), drive shaft torque (T) and power input (W), relative to operation at design point.

Very little previous research on four quadrant axial flow compressor mapping has been performed. Second quadrant positive rotation operation (reverse flow) was investigated by Gamache[1] and subsequently by Gamache and Greitzer [2], for a 3-stage, non-repeating axial flow compressor at mean radius rotor blade Reynolds numbers varying between 1.0×10^5 and 2.0×10^5 . These researchers determined that a discontinuity occurred where the second quadrant characteristic approached zero massflow rate, and that operation in this mode was characterised by strongly three-dimensional, unsteady flow.

Cyrus has conducted research into the third quadrant (reverse rotation) performance of an axial fan[3]. It was found that high rotor blade incidence angles compared with first quadrant operation were necessary in order to operate in the compressor regime, and that a significant degradation of performance occurred, largely due to flow separation in blade rows.

Cyrus [4] also investigated fourth quadrant(turbine-like) operation of the final stages of an industrial axial flow compressor operating at extremely low flow rates and speeds. For this operating mode, Cyrus found that flow separation occurred on the pressure surface, causing large losses. The flow was found to be strongly three dimensional, not corresponding well to two-dimensional cascade data.

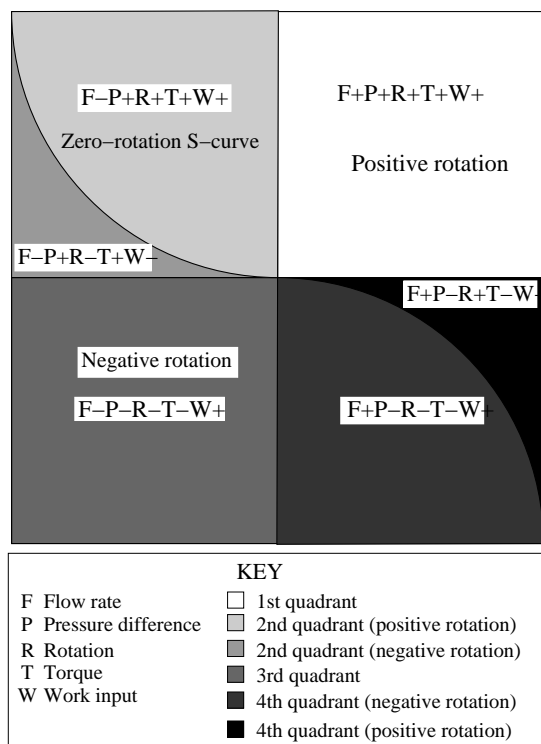


Figure 1: Generic Four Quadrant Compressor Map

EXPERIMENTAL FACILITY

A three-stage axial flow compressor manufactured by the Royston Fan Co. Ltd. was used in the experimental investigation. The machine operates at a design speed of 3000 rpm, with a design mass flow rate of 2.7 kg/s, and a nominal total-to-total pressure ratio of 1.022. The entire operating range of the machine occurs within the subsonic incompressible regime, the first stage rotor having a relative blade-tip Mach-number of 0.2 when operating at design point. The relative rotor blade tip Reynolds number at design point is 1.5×10^5 , although tests were conducted at a reduced speed, due to power limitations, leading to lower Reynolds numbers of the order of 1.25×10^5 . The compressor has 43 rotor blades and 41 stator blades per stage. All stages are repeating and identical. It is fitted with NACA-65 blades on circular arc camber lines with the outflow from the stator blade rows in the axial direction. The reaction ratio of the compressor is approximately 0.82 at design point. The compressor has constant hub and casing diameters of 300 mm and 420 mm. The nominal blade length is 60 mm and the blade chords are 30 mm, with a maximum blade thickness 10 % of that value. The parameters defining the blades are given in Table 1. Spacing between rotor and stator rows in each stage is 22 mm at the mean radius, which is identical to the inter-stage spacing. There are no inlet or exit guide vanes. The compressor is shown in section in figure 2.

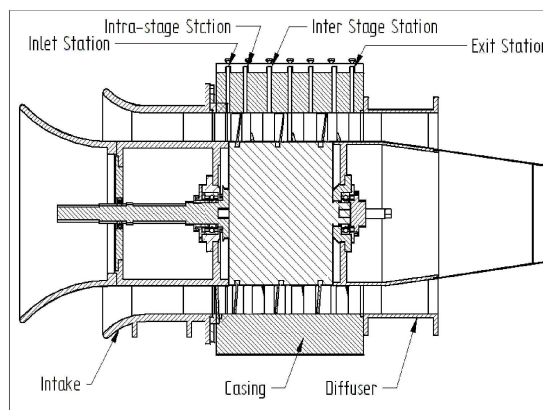


Figure 2: The test compressor in section

The drive system consists of a direct current motor with a thyristor control system. The motor cooling fan exhausts air through an attached duct fitted with an axially aligned honey comb grid to ensure that the cooling air is swirl-free and does not exert a torque on the motor. The flow at the compressor exit is exhausted to a Venturi meter. For first quadrant operation, an adjustable disk throttle is fitted to a threaded spindle mounted on the venturi outlet by means of a three legged spider. This was replaced by an auxiliary fan mounted at the outlet of the venturi-meter, to argument or op-

Blade section radial position (mm)	Blade profile stagger angle (degrees)	Blade profile camber angle (degrees)	Blade row solidity
ROTOR			
150.0	38.00	31.04	1.3051
165.0	45.00	23.48	1.1864
180.0	49.40	17.93	1.0876
195.0	53.00	13.85	1.0039
210.0	56.10	10.90	0.9322
STATOR			
150.0	20.38	46.28	1.3687
165.0	18.18	43.39	1.2443
180.0	16.61	41.05	1.1406
195.0	14.90	40.57	1.0529
210.0	14.32	40.00	0.9777

Table 1: Blade profile data for the Rofanco compressor

pose the compressor in order to access all possible modes of operation. The fan used for these tests was a 483 mm diameter two-stage, contra-rotating Woods axial flow fan, driven by two 4.1 kW induction motors. This fan was mounted at the venturi meter outlet, with honeycomb flow straighteners in between the fan and venturi in order to remove swirl due to the fan. The speeds of both stages of the contra-rotating fan were variable by means of a single frequency control system at frequencies of up to 55 Hz, giving maximum fan speeds of 3170 rpm. A schematic illustration of the experimental setup is shown in figure 3.

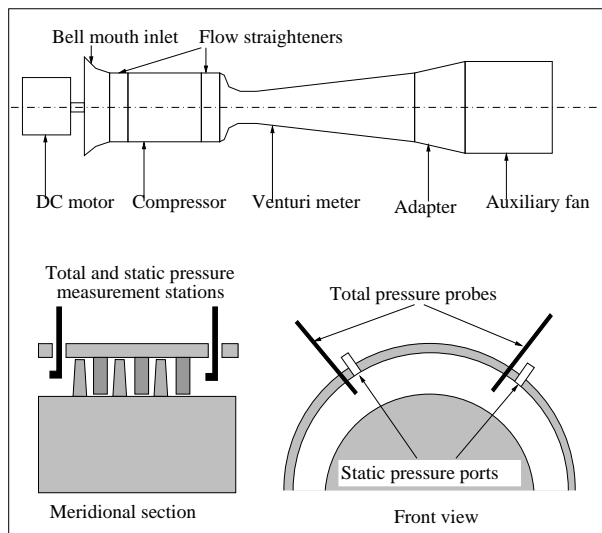


Figure 3: A schematic of the compressor with auxiliary fan

Two three-hole cobra probes were used to determine static and stagnation pressures at the compressor inlet and outlet. The inlet probe has a 5 mm long, 3 mm wide head, while the outlet probe had a head approximately 5 mm long and 5 mm

wide. The probes were traversed across the compressor annulus and static and pressures were determined at six equi-spaced radial positions, for the purposes of averaging across the annulus. Static pressure data was also obtained from tappings at the compressor inlet, immediately upstream of the first rotor row, and at the outlet, immediately downstream of the last stator row. This data was used for comparison and validation of that obtained from the probes.

Pressures from the probes and tappings were recorded by means of eight AutoTran model 860 pressure transducers.

Torque acting on the compressor was measured by means of an HBS 350 load-cell with a nominal load capacity of 20 kg. The combined linearity and hysteresis error for the load-cell was 0.03% of its rated output. The load-cell was connected to a HBM Scout-55 bridge-amplifier. The load-cell is attached to a 320 mm long arm mounted on the side of the compressor motor. The motor housing is mounted on air-bearings which are concentric to the compressor-shaft, allowing the motor to rotate due to the torque generated with very little friction. Data was captured by means of an Agilent 34970A 22-channel data logger.

RESULTS AND DISCUSSION

The total to static and torque coefficient, and efficiency results will now be discussed, quadrant by quadrant, for positive rotation and negative rotation operation. Following Gamache [1], the total to static pressure coefficient ψ_{TS} is defined as follows:

$$\psi_{TS} = \frac{P_{0,inlet} - P_{outlet}}{1/2\rho U^2} \quad (1)$$

for axial flow in the design direction, and

$$\psi_{TS} = \frac{P_{inlet} - P_{0,outlet}}{1/2\rho U^2} \quad (2)$$

for reversed axial flow. The total to static efficiency uses a similarly definition in the pressure difference term. The torque coefficient τ is defined as:

$$\tau = \frac{T}{1/2\rho U^2 d_{tip} A} \quad (3)$$

again following Gamache [1].

First quadrant operation(F+P+N+T+W+)
First quadrant compressor operation has been documented for this machine [5] and others operating in various flow regimes such as subsonic compressible [6] and transonic [7]. Stall inception appears to occur at a flow coefficient of approximately 0.38 (figure 4). Most of the characteristic could be obtained by adjustment of the throttling valve on the compressor, however the auxiliary fan was necessary to access points with a high flow and low pressure coefficient, near the boundary of the fourth

quadrant. The torque coefficient characteristic (figure 5) crosses the x-axis at a higher flow coefficient than the pressure rise coefficient. Between these two points the compressor runs at a negative efficiency. The peak total to static efficiency of the compressor is 66 % (figure 6), lower than that of axial flow compressors employed in aircraft engines or industrial applications. This may be due to three factors, namely:

- the low Reynolds numbers which occur under test conditions
- the nature of the frictional losses associated with the compressor drive system and rotor bearings, the magnitude of which decrease more slowly than that of aerodynamic effects for a given speed decrease
- exit dynamic pressure of the working fluid is not taken into account in total to static efficiency, yielding a lower value than total to total efficiency (although this would apply to all axial flow compressors)

The characteristic determined for the first quadrant is of a similar form to that determined by Gamache and Greitzer[2]. Figure 7 shows the characteristic and some of the data of Gamache and Greitzer[2] for a compressor build with a reaction of 0.74. The most important difference between figure 7 and 4 is perhaps the large degree of hysteresis displayed in the former; this is due to the fact that this phenomenon has not been investigated during this work, although it has been previously investigated for this machine [5].

Second quadrant operation for positive rotation (F-P+N+T+W+)

Second quadrant operation for positive rotation occurs when the pressure difference between the compressor outlet and inlet becomes so large that axial flow occurs in the reverse of the normal direction. This may occur during surge, or as a result of industrial accidents. The unsteady nature of the reversed flow in this mode of operation resulted in unreliable stagnation pressure data at the compressor inlet (a problem also experienced by Gamache [1]). The total to static pressure characteristic for this mode of operation (figure 4) is of a similar shape to that found by Gamache and Greitzer [2] (figure 7), and also exhibits a discontinuity for low negative flow coefficients near the y-axis. This is a highly dissipative mode of operation, in which a maximum temperature increase of 10 K was observed in the working fluid. This equates to 3 kW of power dissipated in the form of heat, which is 60 % of the fluid power at design point. For comparison, the stagnation temperature rise across the machine when operating at design point is approximately 2.5 K. In this mode of operation, where virtually all the fluid power is supplied by the auxiliary fan and most of the energy input is dissipated as heat, efficiency has little meaning, and is consequently

not plotted.

Fourth quadrant operation for positive rotation (F+P-N+T-W-)

Fourth quadrant operation above the S-curve represents a turbine-like mode of operation for the compressor, similar to that investigated in [4]. The massflow rate and consequently the flow coefficient are considerably higher than those occurring in the first quadrant. As can be seen in figures 4 and 5, the pressure and torque coefficient characteristics join smoothly with those of the first quadrant. Total to static turbine efficiency, which is defined as the inverse of compressor efficiency, is presented in figure 6, as the compressor is generating shaft power in this mode.

Second quadrant operation for negative rotation (F-P+N-T+W-)

Second quadrant operation below the S-curve is another turbine-like mode of operation; this time for reverse flow and rotation. The characteristics in figures 8 and 9 are very similar in shape to turbine characteristics, particularly if the pressure coefficient is plotted on the x-axis and the flow coefficient on the y, as is common practice with turbines. The direction of blade curvature is better suited to turbine operation than fourth quadrant operation, however, yielding a higher turbine efficiency of 55 %, as can be seen in figure 10.

Third quadrant operation (F-P-N-T-W+)

In third quadrant operation (F-P-N-T-W+), negative rotation, mass flow rate and pressure difference across the compressor were observed. In this mode the machine operates as a compressor running in the reverse of the normal direction [3]. However, the blades are curved in the wrong direction for such operation, and efficiency is thus considerably lower than for first quadrant operation, as can be seen in figure 10. There is also a larger difference between the flow coefficients at which zero torque and pressure rise occur. This results in rather large efficiencies at high negative massflow rates just below those necessary for turbine operation. However, this is deceptive, as most of the fluid power in this mode is supplied by the auxiliary fan. However, torque must be applied to the compressor by the motor to maintain rotational speed, as can be seen in figure 9.

Fourth quadrant operation for negative rotation(F+P-N-T-W+)

Fourth quadrant operation below the S-curve is a dissipative condition not unlike that occurring for second quadrant positive rotation, although the amount of power dissipated is less for this mode, with a maximum recorded temperature increase of 4 K, compared with 10 K observed for second quadrant, forward rotation operation. As for second quadrant positive rotation operation, efficiency is not plotted on figure 6 for this mode, as it has little meaning.

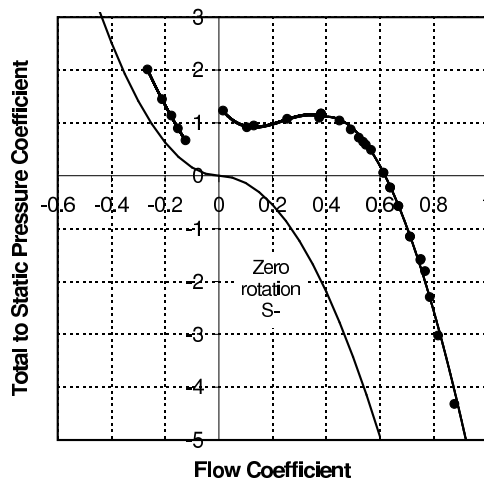


Figure 4: Four-quadrant total to static pressure coefficient compressor map for positive rotation

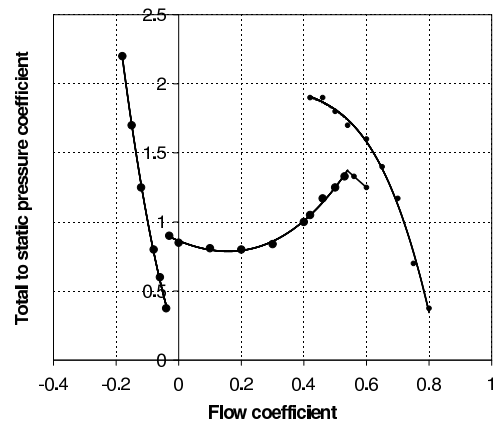


Figure 7: First and second quadrant total to static pressure coefficient map of Gamache and Greitzer[2]

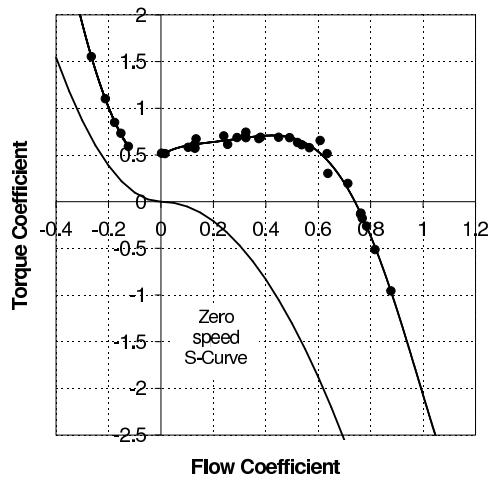


Figure 5: Four-quadrant torque coefficient compressor map for positive rotation

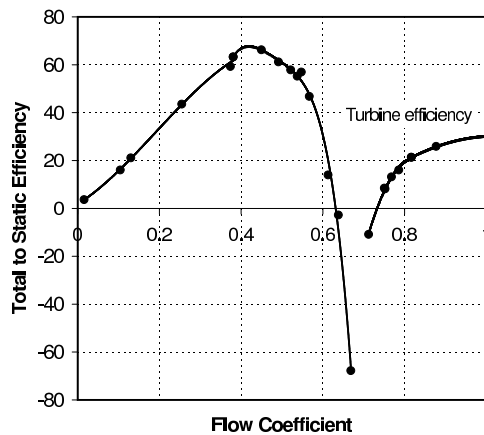


Figure 6: First and fourth quadrant total to static efficiency map for positive rotation

CONCLUSIONS

The non-dimensional characteristics for total to static pressure rise, torque and efficiency of a low speed axial flow compressor were successfully determined for positive and negative rotation in for all four quadrants. Six possible modes of operation were identified and accessed: two compressor-like modes, two turbine-like modes, and two dissipative modes. Zero-speed S-curves for total to static pressure rise and torque were also determined.

Characteristics for first quadrant operation were of the shape expected for this type of machine.

Second quadrant positive rotation operation was a highly dissipative mode of operation, and the working fluid increased in static temperature by as much as 10 K. This mode of operation would thus be dangerous for machines operating at higher speeds.

In the second quadrant, negative rotation turbine mode, the test compressor displayed a total to static turbine efficiency of approximately 55 %.

The fourth quadrant turbine efficiency was approximately 30 %. Second quadrant turbine efficiencies will be considerably higher than those of the fourth quadrant for virtually all compressors, as the curvature and shape of compressor blades are much more appropriate for the former than the latter.

Fourth quadrant negative rotational operation was dissipative in nature, but the temperature rise in the working fluid for this mode of operation was negligible.

Third quadrant operation represents a badly designed compressor with the blades curved in the wrong direction operating in reverse rotation and axial flow. Consequently the compressor is thought to operate in a stalled condition throughout this quadrant, yielding low efficiencies.

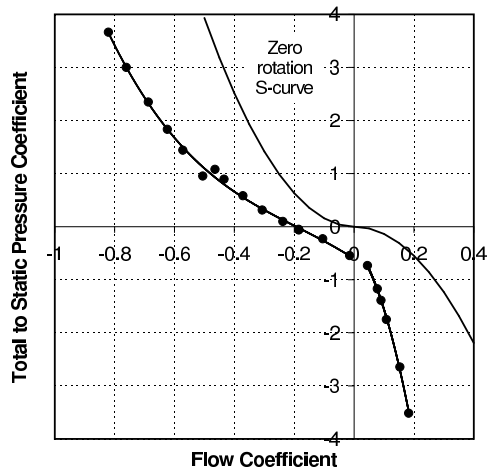


Figure 8: Four-quadrant total to static pressure coefficient Map for negative rotation

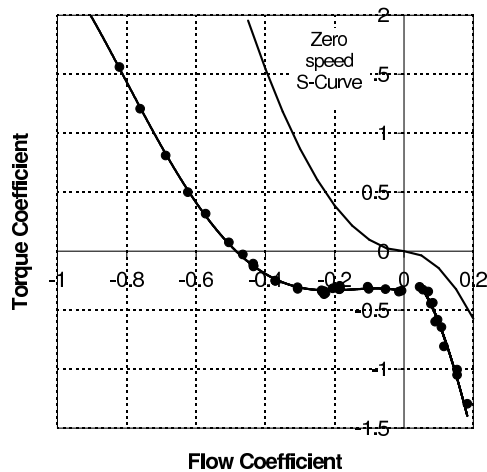


Figure 9: Four-quadrant torque coefficient map for negative rotation

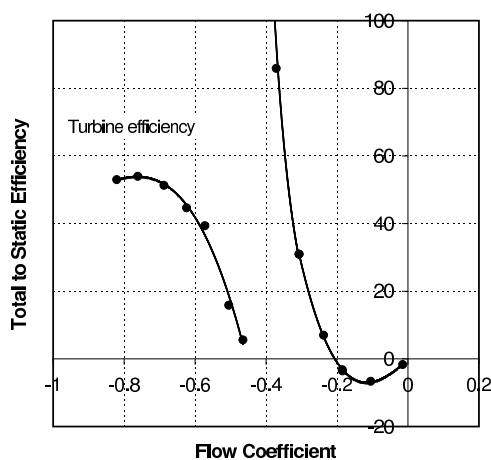


Figure 10: Second and third quadrant total to static efficiency map for negative rotation

Acknowledgements

The authors would like to thank M. Bailey for his assistance in preparing the experimental rig, and the CSIR/Defencetek for funding this research.

References

- [1] R.N. Gamache. *Axial Compressor Reverse-Flow Performance*. Ph.d. dissertation, Massachusetts Inst. of Technology, Cambridge, MA., May 1985.
- [2] R. N. Gamache and E. M. Greitzer. Reverse flow in multistage axial compressors. *International Journal of Turbo and Jet Engines*, 6:461–473, 1990.
- [3] Vaclav Cyrus. Axial fan at reverse flow. *Proceedings of ASME Turbo Expo 2004: Power for Land, Sea and Air*, pages 437–446, 14-17 June 2004.
- [4] Vaclav Cyrus. The turbine regime of a rear axial compressor stage. *ASME Gas Turbine and Aeronengine Congress and Exposition, Brussels, Belgium*, pages 1–8, 11-14 June 1990.
- [5] T.H. Roos. A prediction method for flow in axial flow compressors. Master's project, University of Stellenbosch, Department of Mechanical Engineering, Faculty of Engineering, March 1995.
- [6] R. E. Budinger and A. R. Thompson. Investigation of a 10-stage subsonic axial-flow compressor; II—preliminary analysis of overall performance. NACA Research Memorandum RME52C04, NACA, Washington DC, 1952.
- [7] K. Kovach and D. M. Sandercock. Experimental investigation of a five-stage axial-flow compressor with transonic rotors in all stages; II—compressor overall performance. NACA Research Memorandum RME54G01, NACA, Washington DC, 1954.